

RSC Advances



This is an *Accepted Manuscript*, which has been through the Royal Society of Chemistry peer review process and has been accepted for publication.

Accepted Manuscripts are published online shortly after acceptance, before technical editing, formatting and proof reading. Using this free service, authors can make their results available to the community, in citable form, before we publish the edited article. This *Accepted Manuscript* will be replaced by the edited, formatted and paginated article as soon as this is available.

You can find more information about *Accepted Manuscripts* in the [Information for Authors](#).

Please note that technical editing may introduce minor changes to the text and/or graphics, which may alter content. The journal's standard [Terms & Conditions](#) and the [Ethical guidelines](#) still apply. In no event shall the Royal Society of Chemistry be held responsible for any errors or omissions in this *Accepted Manuscript* or any consequences arising from the use of any information it contains.

**Development and characterization of electrospun mat from Eri silk fibroin and PLA blends
for wound dressing application**

Kuberasampathkumar Shanmugam,^a Subramanian Sundaramoorthy ^{*a}

^a Department of Textile Technology, Anna University, Chennai 600025, India.

* Corresponding author

S. Subramanian

Department of Textile Technology

Anna University

Chennai 600025

India.

Ph: 044-22359247; Fax: 044-22352642

E-mail address: ssubbu@annauniv.edu, ssresgroup12@gmail.com

ABSTRACT

The research is being carried out worldwide on development of multilayer wound dressing systems with each layer satisfying the requirements of ideal wound dressing system for achieving better wound heal performance. In this paper, the mats were prepared from Eri silk fibroin (ESF) and its blend with Poly L-lactic acid (PLA) polymer by the electrospinning process and evaluated for properties those are required for skin contact layer of wound dressing system. Tetracycline hydrochloride (TCH) was added with the polymer solution and was spun into mat. The ESF fibres had a mean diameter of 320 nm and ESF, PLA blend (ESF-PLA) fibres had 502 nm. Phosphate buffer saline (PBS) uptake was lesser for ESF-PLA mat compared to that of 100% ESF mat. The contact angle with water was 23° for ESF mat and 79° for ESF-PLA mat. The vapour transmission rate was lower for ESF-PLA mat compared to that of 100% ESF mat, however, they were found to be lesser than the level at which dehydration would occur. TCH loaded mats showed effective zone of inhibition against gram positive and gram negative bacteria. Cytotoxicity study on neuroblast cells showed that ESF mat did not impair the growth of cells. The *in vivo* study on rat model showed that the wound healing performance of mats developed from 100% ESF and ESF-PLA were better compared to the conventional open wound and gauze cloth wound dressing systems.

Keywords: Antimicrobial, Cytotoxicity, Eri silk fibroin, PLA, Wound dressing, Wound healing.

1. Introduction

A wound is a break in the epithelial integrity of the skin and may be accompanied by disruption of structure and function of underlying normal tissue. Wound healing is a well-orchestrated and complex process which is triggered by tissue injury and ends by regeneration or repair. The process of wound healing is same for all wounds, but rate of healing depends on type of wound, age and immune system of human body, and conditions for healing.¹ The healing of wounds depends not only upon medication but also upon the use of proper dressing techniques and suitable dressing materials. The wound dressing should be able to create the optimal environment for wound healing and should be designed to reduce nursing time by requiring fewer dressing changes. Modern wound dressing theory suggests that an ideal wound dressing should promote exudates absorption, promote gaseous exchange, insulate wound against temperature extremes, provide bacterial barrier, be non-adherent to the wound bed, which allow the dressing to be changed with minimal trauma to the fragile and newly formed epithelium, not be discomfort to the patient, allow conformation to the body contours and prevent formation of eschar.^{2,3} Different types of wound dressings based on single layer gauze cloth, thin films, polyurethane foams, hydrocolloids, hydro gels, alginate, activated charcoal cloth with silver alginates, chitosan and alginate-collagens are available in the market.^{2,4} They have some advantages and limitations and do not completely meet the requirement of ideal wound dressing.^{2,5,6} The worldwide research on development of multilayer wound dressings with each layer satisfying the requirements of ideal wound dressing system is in progress. The present work aims to develop skin contact layer of the multilayer wound dressing system. The skin contact layer is expected to promote exudates absorption or percolate the exudate to the

secondary layer, promote gaseous exchange, keep wound site without contamination and be non-adherent to the wound bed which allow the dressing to be changed with minimal trauma.

Silk is biocompatible and hemocompatible and its scaffold has been successfully used in wound healing because of the presence of amino acids like arginine, glycine, and aspartic acid which helps in the remodeling of epithelial tissues.^{7,8} The research on application of mulberry (*Bombyx mori*), a cultivated silk, as biomaterial has been carried out by many researchers. However, the studies on application of Eri (*Samia Cynthia ricini*), a wild silk, as biomaterial are limited. It was found that the cell attachment, binding, and spreading of L6 fibroblast cells on the Eri silk fibroin (ESF) scaffold were found to be better than those on the mulberry silk fibroin, and the cell viability was also found to be better on ESF scaffolds.^{9,10} The biopolymer, poly L-lactic acid (PLA) shows excellent wicking ability, fast water spreading and rapid drying capability which results the fibres to have a very positive inherent moisture management characteristic. It has additional properties such as thermal insulation, breathability, and water vapor transport properties and buffering capacity to liquid sweat than that of polyester and cotton.¹¹ It is a kind of biodegradable materials with low toxicity, excellent biocompatibility and *in-vivo* bio-absorbability. It is being used in the biomedical applications such as sustained drug delivery systems and implants for orthopedic devices due to its low hydrophilicity. It has low contact angle which would promote low adherence to the wound site.¹² Hence, in the present work, ESF and PLA were used as the material for developing skin contact layer of the wound dressing system.

Electrospinning is a simple and effective method for producing fibres from tens of nanometers to micrometers.¹³ Electro spun mats have huge surface area per unit mass and its micro porous structure could quickly attract fibroblasts to dermal layer.^{14,15} The wound dressing

materials produced by electrospinning technology have special properties such as hemostasis, absorbability, semi-permeability, conformability, functional ability and scar-free compared to the dressings produced by conventional methods.^{13,16} Hence, in the present work, the mats were produced from 100% ESF and blend of ESF-PLA by electro spinning method. Tetracycline hydrochloride (TCH) was added with the polymer of 100% ESF and ESF-PLA and the mats were prepared. They were characterized for physical, chemical and biological properties which are required for using them as a skin contact layer of multilayer wound dressing system.

2. Materials and Methods

2.1. Preparation of the wound dressing

Eri silk (Central Silk Board, India), PLA, Chloroform (99%, SRL India) and Tri-flouro acetic acid (TFA) (99%, SRL India) were used to prepare the polymer solution and Tetracycline hydrochloride (TCH) (95%, Sigma Aldrich) drug was used as an antibacterial agent. The Eri silk was degummed with sodium carbonate solution boiling at 75°C and at a pH level maintained at 8.5-9.0 for 30 min to remove sericine from the silk filament. The polymer solution was prepared by dissolving a mixture of ESF and PLA in different ratios viz., 87.5:12.5 and 100:0 in a solvent containing mixture of chloroform and TFA (30:70). TCH was added with this polymer solution in the concentration of 1%, 2%, and 3% (w/v) to prepare the samples with antibiotic effect. The polymer solution was taken in a 2ml syringe pump having a needle diameter of 0.55 mm. The syringe was fixed on the infusion pump in vertical position. The distance between the syringe pump and collecting drum was kept at 15 cm, and a 20 kV supply was applied between the syringe pump and collecting drum. The flow rate of the solution was maintained at 1.0 ml per hour. The concentration of polymer solution and the electrospinning parameters were optimized

such that there was no spraying of solution or beads formation. The mat was electrospun at a concentration of 13 % (w/v) of polymer in solvent.¹⁷

2.2. Physical and Chemical Characterization

2.2.1. Surface and functional

The electrospun mats were characterized using Scanning Electron Microscope (SEM) (Hitachi, S-3400N). From the SEM image, the diameter of the fibres was measured using ImageJ software. The mats electrospun from 100% ESF, ESF-TCH blend, 100% PLA, PLA added with TCH were analyzed for functional groups using FTIR spectroscope (Bruker, tensor 27) to examine the presence of TFA and TCH in the mat after electrospinning.

2.2.2. Friction and surface roughness

Kawabata's Evaluation System FB4 (KES-Kato Tech., Japan), which is designed to measure the surface properties of textile fabrics, was used to measure the friction and surface roughness properties of mat in terms of geometrical roughness (SMD), the frictional coefficient (MIU) and the mean deviation of the coefficient of friction (MMD). The study was conducted to assess the effect of drug loading on the friction and surface roughness of mat. Fifteen tests per sample were conducted and its average was taken.

2.2.3. Contact angle

The wound dressing should facilitate ease of application and removal, and also proper adherence so that there will not be any area of non-adherence left to create fluid-filled pockets for proliferation of bacteria.¹⁸ The produced nanofibrous mats were analyzed for hydrophilicity as per a Krüss Easy Drop method using an optical measurement system (M/s Kruss GmbH, Germany). This system is equipped with a high precision liquid dispenser to precisely control the drop size of the liquid used. A drop of distilled water of 2 μ l was placed on the electrospun mat.

The image of the water drop was captured and stored using a monochrome interlined CCD video camera, a PC-based acquisition and data processing software, provided with the instrument.

2.2.4. Phosphate buffer saline (PBS) absorption and transmission rate

In a wound environment, the exudates and other fluids coming out of the wound need to be absorbed to hasten the healing process. The rate of absorption of the exudates and retention are the significant factors for quick healing of the necrotic tissues in the wound. Moreover, the autolytic debriment of the wound protects newly formed cells and facilitates angiogenesis and the re-epithelialization is promoted by quick absorption.¹⁹ The wound dressing should remove excessive exudates from the wound site and should permeate it to the outer surface which may either be absorbed by secondary layer or be evaporated if exposed to atmosphere. The PBS uptake capacity of ESF and ESF-PLA mat was determined by immersing a known weight of nanofibrous mat in PBS maintained at a pH of 7.4 and 37⁰C. The dry weight of the mats was measured (W_d). They were kept in the solution for a period 30 min and measurement of weight of the samples was carried out at different intervals. Before weighing, the sample was placed on the tissue paper to remove excess amount of solution present on the surface of the mat. The percentage of the PBS solution absorbed by the sample was calculated by using the Equation 1.

$$\text{Equilibrium PBS content (\%)} = \frac{[W_w - W_d]}{W_w} \times 100 \quad (1)$$

W_d = Dry weight of the sample

W_w = Swollen weight of the sample

The ability to control loss of moisture from a wound is commonly determined by the moisture vapor permeability of the dressing or dressing system.²⁰ PBS transmission rate of the mat was determined as per ASTM E96-00 (WVTR).²¹ The test was conducted in an environmental chamber maintained at temperature of 37⁰C and 35% RH. A container was filled

with known quantity of PBS maintained at pH of 7.4. The test sample and size of the exposing area were maintained at the levels as specified in the standards. The loss in weight of PBS was measured as a function of time and the vapor transmission rate (VTR) was calculated using the following Equation 2.

$$VTR = \frac{\text{slope} \times 24}{A} \text{ g/m}^2/\text{day} \quad (2)$$

where, A is test area of the sample in m^2 .

2.3 Biological Characterization

2.3.1. Antibacterial and cytotoxicity

The antibacterial activity of the Tetracycline hydrochloride incorporated 100%ESF and ESF-PLA mats against Gram negative bacteria *Escherichia coli* and *Pseudomonas aeruginosa* and Gram positive bacteria *Staphylococcus aureus* and *Staphylococcus epidermidis* were studied as per disc diffusion (CLSI, 2001) method. These four bacteria are commonly found in the wound site.²²⁻²⁴ A 25 ml of molten Mueller Hinton Agar was poured into a Petri plate and was allowed to solidify. After 18 hours, 100 μl of pathogenic bacteria cultures were transferred onto a plate and culture lawn was made by using sterile L-rod spreader. After 5 min, the nano fibrous mats of uniform diameter were placed on the culture plates. The plates were incubated at 37°C for 24 h. The antimicrobial activity was determined by measuring the diameter of the zone of inhibition around the mat using antibiotic zone scale (Himedia, Mumbai, India). Three tests were conducted per sample, the average and the standard deviations were determined.

Cytotoxicity was assessed by MTT assay using Mouse neuroblastoma Neuro-2A cell line obtained from NCCS, Pune, India. Since, the Mouse neuroblastoma cell line is sensitive to the morphology and nature of polymer, and alignment of fibers in the mat it was selected for the cytotoxicity study. The cell line was maintained in DMEM with 10% FBS (HIMEDIA-RM112),

200 mM Glutamine, 50 mg/ml gentamycin (SIGMA-G1272) and 2 mg/ml of amphotericin B (SIGMA- A2942), in a humid atmosphere of 5% (v/v) CO₂ and 95% (v/v) air at 37 °C. The expanded Neuro-2A cells (70-90%) were plated in 48 well cell culture plate at a seeding density of 2000 cells/cm² per well. The test was executed with cells overlaid upon electrospun mat and incubated for 18 hours. The cells were incubated for another 3 h in 15 µL MTT stock solution (5 mg/mL) and the assay content was transferred to 96 well plate. The absorbance was read at 570 nm using spectrophotometric microplate reader.

2.3.2 *In vitro* blood compatibility

Blood compatibility is one of the most important properties of biomedical materials. Hemolysis is the rupture of erythrocytes and release of their contents into surrounding fluid. The electrospun mates were subjected to a hemolysis assay to assess their blood compatibility. Human blood was collected from a healthy volunteer and was placed in a 3.8% sodium citrate-coated tube. Then it was diluted with PBS (pH 7.4) at a ratio of 1:20 (v/v). The test samples were autoclaved and then they were immersed in 100 µl of blood-PBS solution followed by incubation at 37°C for 60 min. Then the samples were spun at 3,000 rpm for 10 min. The optical density value (OD) of the supernatant was measured using a UV spectrophotometer at 545 nm. The blood diluted with PBS was taken as negative control, and the blood with Sterile Water for Injection (SWFI) was taken as positive control, and the hemolysis percentage was estimated using the following equation 3.²⁵ Three tests were conducted per sample and the average was taken.

$$\% \text{ Hemolysis} = \frac{\text{OD for the test sample} - \text{OD for the negative control}}{\text{OD for the positive control} - \text{OD for the negative control}} \times 100 \quad (3)$$

2.4. *In vivo* wound healing performance

2.4.1. *Experiment*

The wound healing performance of the mats was evaluated using rat model. Thirty six Male Wistar rats weighing approximately 250g/rat were used for the experiment with 6 rats in 6 groups. Rats were anesthetized by intramuscular injection of Ketamine at a dosage of 20mg/kg body weight. The skin of the animal was shaved by razor and disinfected using 70% ethanol and marked a size of $1.5 \times 1.5 \text{ cm}^2$. Partial thickness wound was excised at the back side of the rat using sterile surgical blades (CE 0197 Swan, Japan). Group1 (G1) wounds were kept open without any dressing material or any ointment. For Group2 (G2) wounds, the commercially available Povidone-iodine based ointment (Betadine) was applied evenly on the wound site with the aid of fire-polished glass rod tip. The same procedure of G2 was followed for Group3 (G3) wounds, but additionally, it was covered with sterile gauze cloth and then fixed with elastic adhesive bandage (Dynaplasts) to prevent dislodging or peeling off of dressing by rat. Group4 (G4) and Group5 (G5) wounds were covered with mats produced from 100% ESF with TCH and ESF-PLA with TCH mats respectively and then fixed with adhesive bandage. Group6 (G6) wounds were covered using hydrocolloid dressing that is available commercially. After dressing, all the animals were kept in separate cages in an air-conditioned room (temperature, $25 \pm 1^\circ\text{C}$; relative humidity, $50 \pm 10 \%$) for 12 hr light/dark cycle and were fed with commercial rat feed and water until they were sacrificed. The tissues from wound sites were collected on the 3rd, 7th and 11th days of experiment and were stored in 10% formalin for Hematoxylin–Eosin (HE) staining for histological observation. The wound dressings and adhesive tapes were changed for

first time on 3rd day and then they were changed on every alternate day during the complete study i.e. up to 17 days.

2.4.2. *Clinical Evaluations*

Clinical observation of animals of all groups was done daily during the healing performance study. The wound site was traced in a transparent film to measure the size of the wound area and the clinically observable changes in the wound such as inflammation, exudation, re-epithelialization, granulation and wound contraction were imaged.

3. Results and discussion

3.1. *Surface and functional characters*

The SEM image and fibre diameter histogram of the electro spun mats produced from 100% ESF and 87.5: 12.5% ESF-PLA with and without TCH are given in Figs. 1a-1dd. The Figures show the nano fibrous mats without beads produced by electro spinning from 13% conc. polymer solution. In the case of 100% ESF mat without TCH, the average diameter is found to be 320.4 nm with standard deviation (SD) of 153.9 nm, whereas, the average is 502.6 nm and SD is 205 nm for ESF-PLA mat without TCH. In the case of 100% ESF mat with TCH, the average fibre diameter is 605.3 nm and SD is 185.2 nm, whereas, the average is 640 nm and SD is 121.3 nm for the ESF-PLA mat with TCH.

It can be seen from the SEM images 1a-b that incorporation of PLA with ESF does not affect the surface characteristic of fibres, however, the diameter of the fibres has increased due to PLA. Figure 1c and 1d respectively show the SEM image of ESF mat, ESF-PLA with TCH. The beads are not created due to incorporation of TCH with the polymer. Significant increase in diameter is found in the following cases: (i) Addition of PLA with ESF without TCH (p value

1.8×10^{-7}), (ii) Incorporation of TCH with ESF (p value 1.11×10^{-16}), (iii) Incorporation of TCH with ESF-PLA (p value 6.16×10^{-5}). However the difference is not significant between ESF with TCH and ESF-PLA with TCH.

The FTIR spectra of the 100% PLA electrospun mat, 100% Tetracycline hydrochloride drug in the form of powder and PLA with TCH mat are shown in Figures 2a-c respectively. In the Fig. 2c, stretching vibrations at 3301 cm^{-1} is due to the presence of N-H group, stretching vibrations at 2993, 2970 and 2931 cm^{-1} show the presence of C-H. The bending modes of C-H are shown at 1448 and 1365 cm^{-1} . The peaks at 1713 cm^{-1} and 1524 cm^{-1} show the presence of carbonyl C=O group and amino groups of amide in ring respectively. The C-N stretching vibrations at 1195 and 1068 cm^{-1} and O-H stretching vibrations at 3655 cm^{-1} appearing in Fig. 1c confirms the presence of drug in the mat. FTIR spectra of 100% ESF without TCH and with TCH are shown in Fig. 2d-e respectively. In the Fig. 2e, N-H stretching vibrations at 3301 cm^{-1} , C-H stretching vibrations at 2970 and 2931 cm^{-1} , C-H bending modes at 1450 and 1357 cm^{-1} , the carbonyl C=O group peak at 1743 cm^{-1} and C-N stretching vibrations at 1041 cm^{-1} , also confirm the presence of the drug.²⁶⁻³⁰ In the Figures 2d-e, it can be noted that stretch band $1100 - 1200 \text{ cm}^{-1}$ pertaining to TFA used for preparing the polymer solution, which may be allergic, is not present in the nano fibrous mat.¹⁰

3.2. Friction and surface roughness

To study the effect of drug on the friction and surface roughness, the 100%ESF nano fibrous mats with TCH and without TCH were chosen as the representative samples. The MIU, MMD and SMD values of the ESF mat with and without TCH are given in Table 1. There is no significant change in the MIU, the coefficient of friction (p value 0.937) due to the incorporation of drug, which indicates that the friction of the mat is not affected. However, SMD, the

geometric roughness decreases significantly (p value 6.93×10^{-10}) due to incorporation of drug. This is attributed to the deposition of drug on the surface of fibres and also filling up of gap between the fibres. The addition of TCH would not hinder the cell proliferation as there is no increase in coefficient of friction or the geometric roughness due to addition of TCH.

3.3. Phosphate Buffered Saline Uptake and contact angle

The PBS uptake (%) of the 100% ESF and ESF-PLA mats are shown Fig. 3. The mat absorbs the water immediately on contact and reaches saturation level within 5 to 10 seconds. However, it can be seen from the figure that the PBS uptake is lesser for ESF-PLA mat compared to that of 100% ESF mat, which implies that the mat becomes hydrophobic with the incorporation of the PLA. Higher the PBS uptake, the ability to absorb body fluids by the mat will also be higher. The above results can be correlated with the contact angle results as shown in Fig. 4. Figures 4a-b show the contact angle of 100% ESF, ESF-PLA mats respectively. The figures show that contact angle increases from 23° to 79° with the addition of PLA. The 100% ESF mat wets immediately due to its higher hydrophilic character and incorporation of PLA decreases its hydrophilicity. The study indicates that adherence of exudates on the ESF-PLA mat would be lesser than that of 100% ESF mat.

3.4. Phosphate buffer saline transmission rate

A wound dressing applied on the wound should not impair the healing, but protect the wound from secondary infection arising out of the dehydration. The PBS loss of 100% ESF and ESF-PLA with respect to time is shown in Fig. 5. It can be seen from the figure that the vapor loss (g) across the electrospun mat decreases when PLA is added with the ESF. The decrease in VTR is due to hydrophobicity of PLA and its poor absorption of PBS vapour, resulting low transfer of the PBS vapour across the mat. The diameter of the fibre is less in the case of 100%

ESF mat. Smaller diameter results more number of smaller pores and cause increases in void to capillary, which result better wicking and vapour transmission rate. The vapour permeability of commercial wound dressings namely Gelliperm (Geistlich, Switzerland) and Vigilon (Bard Crawley, UK) were found to be 9009g/m²/day and 9360 g/m²/day respectively.³¹ For the hydrogel of alginate and gelatin, it was found to be 2686 g/m²/day,³² and for the asymmetric chitosan membrane, it was ranged from 2109-2792 g/m²/day.³³ The vapor transmission of a wound dressing should prevent excessive dehydration and also buildup of exudate. It has been well documented in the literature that the evaporative water loss for normal skin is about 204 g/m²/day and that for injured skin, it can range from 279 g/m²/day for a first degree burn to 5138 g/m²/day for granulating wound. It was recommended that a rate of 2000-2500 g/m²/day would provide an adequate level of moisture without risking wound dehydration³⁴. The present study shows that the VTR of 100% ESF is 1323 g/m²/day and that of ESF-PLA mat is 835 g/m²/day. The results indicate that the wound dressing developed from the blend of ESF-PLA has lower vapour transmission rate and can maintain a proper moisture level at the wound site. The VTR of 100% ESF is also less than the level which would cause dehydration. The results also show a positive indication for the mat being used in burn wounds, where the water vapor transmission loss is higher and heavy loss of water from the body by exudation and evaporation would lead to a fall in body temperature and increase in the metabolic rate.³²

3.5. Antimicrobial studies

In the Fig. 6 and 7, A1, A2, A3 indicate 1%, 2% and 3% (w/v) of TCH in 100% ESF, B1,B2, B3 indicate 1%,2% and 3% (w/v) of TCH in ESF-PLA mats respectively. C indicates

control sample of 100% ESF without TCH in A grouping and ESF-PLA mats without TCH in B grouping. Figure 6 shows antibacterial activity against gram positive (*Staphylococcus aureus*, *Staphylococcus epidermidis*) and Fig. 7 shows the antibacterial activity against gram negative (*Escherichia coli*, *Pseudomonas aeruginosa*) bacteria. From the figures, it can be seen that the TCH loaded mats show effective zone of inhibition against *S. aureus*, *S. epidermidis* and *E. coli*. Zone of inhibition is not formed in the case of *P. aeruginosa* as it is known that TCH will not be active against *Pseudomonas aeruginosa* bacteria.^{6,35,36} The mean and standard deviation of zone of inhibition values are given in Table 2. The high zone of inhibition confirms the broad spectrum of activity of TCH against both the pathogens and it also proves that the mat does not hinder the release of drug from its surface. The tetracycline drug works by binding specifically to 30s ribosomes of the bacteria thereby preventing the attachment of aminoacyl tRNA to the tRNA – ribosome complex and it also simultaneously inhibits other steps of protein biosynthesis.^{37,38}

3.6. Cytotoxicity

The result of cytotoxicity study carried out using Mouse neuroblastoma cell line is presented in Fig. 8. The results show that the 100% ESF mat supports cell proliferation (100% live cells), where as the ESF-PLA mat shows only 65.4% live cells. The histological sections of the samples are given in Fig. 9. The optical microscope images of the cells seeded on the mat show morphology to that of the control cells used for the study. These images confirm that the silk mat is not inhibiting the growth of cells. It can be seen from the figures that the cells have migrated and are uniformly distributed across the mats.

3.7. Blood compatibility

Table 3 shows the hemolysis% of 100% ESF and ESF-PLA mat with TCH and without TCH. The results show that hemolysis% increases with increase in TCH. The 100% ESF mat

with TCH has lesser hemolysis % than ESF-PLA mat with TCH. However, the hemolysis% is less than 5% in all the cases, which indicate that all the samples are blood compatible. Hence, 100% ESF as well as ESF-PLA mats can be used as skin contact layer for wound dressing applications.

3.8. Clinical examination

Photographs of wounds of six groups of animals (segregated based on the dressing procedure) taken on 0, 3,5,7,9,11,13,15 and 17th day of the post operation are shown in Fig. 10. The clinical examination was carried out only upto 7th day of post operation as there was no difference on the wound surface between the groups after 7th day, except the area of wound site. However, pathological study was conducted up to 11th day. The decrease in area of wound on different days of post operation for all the groups is given in Table 4. The average and standard deviation of wound size measured from wound site of rats alive during the time of measurement are given in the table. The observations are presented as follows.

3.8.1. Third day observation

In Group1 (G1), where the wound was kept open without any dressing material or any ointment, the wound was found to be hemorrhagic and scab was present on the open wound area. Group2 (G2), the wound applied with betadine and Group3 (G3), the wound applied with betadine and covered with gauze cloth also showed similar observations as found with G1, but some cotton fibres were adhered on the wound site of G3. In the case of Group4 (G4), the wound dressed with 100% ESF with TCH mat, and Group5 (G5), the wound dressed with ESF-PLA with TCH mat, it was observed that the nano fibrous material had uniformly adhered to the freshly excised wound site and the yellow color showed the release of the drug on to the wound surface. It was also observed that the wound site was clean in pinkish red color without any

excess exudates at the wound surface. In Group6 (G6), the wound dressed with hydrocolloid based wound dressing, the dissolved hydrocolloid was found on the wound site which may be due to dissolving of gelatinous material present in the hydrocolloid by exudates. The removal of this gelatinous material may damage the new epithelial cells and it may delay wound healing.³⁹ In all the six groups, neither infection of wound nor the re-epithelialization was observed.

3.8.2. Fifth day observation

Exudates and bacterial colonies were found in the G1 wounds due to infection by foreign bodies. In G2, some wounds were found to be hemorrhagic and scab was present on the wound site. G3 wound showed adherence of cotton fibre on the wound site and it damaged the newly formed epithelial at the time of redressing. In G4 and G5 wounds, collagen fibres were formed at the margin of the wound and epithelial cells proliferate continuously to cover the wound from margin and the size of the wound got reduced up to 16 %.

3.8.3. Seventh day observation

G1 and G2 wounds showed starting of re-epithelialization and the wounds of G4 and G5 rats showed reduced wound area compared to that of 5th day wounds. G6 showed that the epithelium was orderly covered and the wound area contracted upto 32%. It can be observed from the table that size of wound reduces in all the groups as the number of days after post-operation increases.

3.8.4. Seventeenth day observation

At the end of 17th day, the wound of G4, G5 and G6 healed completely as against the wounds of G1, G2 and G3. It proves that the wound healing efficiency of dressings used in G4, G5 and G6 are better than other three.

3.9. Histological observation

3.9.1. Group1

The histopathological photograph of G1 wounds (open wound without ointment or dressing) on 3rd, 7th and 11th day of post-operation is shown in Fig. 11. On the 3rd day, the section studied from the wound skin showed chronic inflammation with collagen and the stroma appeared edematous. There was no evidence of fibrosis or healing of wound. On 7th day, the skin showed full of acute ulcer. The granulation tissue with chronic inflammation was found. The inflammation was found to be composed of neutrophils and nuclear debris. On 11th day of observation, the open wound skin showed epidermis with granulation tissue. The granulation tissue with areas of thick fibrosis proceeding towards scar formation was noted.

3.9.2. Group2

The histopathological photograph of G2 wounds (applied with betadine, but without dressing) on 3rd, 7th and 11th day of post-operation is shown in Fig. 12. On the 3rd day, the section studied from the skin at wound site showed chronic inflammation composed of lymphocytes and plasma cells. The stroma appeared edematous and granulation tissue was not seen. There was no evidence of fibrosis or healing of wound. On 7th day, the section studied from skin showed late granulation tissue with few chronic inflammatory cells. The granulation tissue with fibrosis and fibroblasts were also noted. On the 11th day of observation, the skin showed granulation tissue

with some inflammatory cells. The subcutaneous tissue with fibroblasts and increased fibrosis were also seen. The granulation tissue was slowly replaced by fibrosis.

3.9.3. Group3

The histopathological photograph of G3 wounds (applied with betadine and dressed with gauze cloth) on 3rd, 7th and 11th day of post-operation is shown in Fig. 13. On the 3rd day, the section studied from skin at wound site showed granulation tissue composed of inflammatory cells and nerve bundles. The capillary proliferation and hemorrhage were also noted. On 7th day observation, the skin showed acute inflammation with collagen. The stroma appeared edematous. There was no evidence of fibrosis or healing of wound. On 11th day, the skin showed granulation tissue with plenty of fibroblasts and few capillaries with dense healthy fibrosis and there was evidence of healing of wound.

3.9.4. Group4

The histopathological photograph of G4 wounds (dressed with 100% ESF and TCH mat) on 3rd, 7th and 11th day of post-operation is shown in Fig. 14. On the 3rd day, the section studied from skin showed unremarkable epidermal skin with sebaceous glands. The hair follicles and the granulation tissue were also present. The underlying region showed minimal necrosis with inflammation. On 7th day, the skin showed acute ulcer with dense and older granulation tissue. Areas of fibroblasts and fibrosis were seen. The capillary proliferations were also noted. The 11th day observation showed dense fibrosis with scattered fibroblasts and overlying skin, and there was evidence of healing of wound.

3.9.5. Group5

The histopathological photograph of G5 wounds (dressed with ESF-PLA and TCH mat) on 3rd, 7th and 11th day of post-operation is shown in Fig. 15. On 3rd day, the section studied from

skin showed predominantly acute ulcer composed of neutrophils and nuclear debris. There was no evidence of fibrosis or healing. On 7th day, the skin showed some older granulation tissue with adjacent skin adnexa. There was acute inflammation composed of neutrophils. The subcutaneous with fibrosis and fibroblasts were also noted. On 11th day, the skin showed well formed granulation tissue with thick fibrosis, and few scattered fibroblasts and capillaries. The progress of wound healing was found to be lesser compared to G4.

3.9.6. Group6

The histopathological photograph of G6 wounds (dressed with hydrocolloid based wound dressing) on 3rd, 7th and 11th day of post-operation is shown in Fig. 16. On the 3rd day, the section from the central core wound was found with acute inflammatory cells. The granulation tissue with adjacent inflammation was seen in the subcutaneous fat and dermis. On 7th day, the section from the skin showed acute necrotic slough with older granulation tissue. The granulation tissue with areas of fibrosis and fibroblasts were also seen. Mixed acute and chronic inflammations were seen. On 11th day, the section studied from skin showed older granulation tissue with kinky fibroblasts and dense fibrosis. Mixed inflammatory cells and capillaries were also seen.

The studies show that electrospun mats of 100% ESF with TCH, ESF-PLA with TCH and the hydrocolloid based dressing can be used as skin contact layer of wound dressing system. However, it is to be noted that dissolving of materials present in the hydrocolloid based dressing may contaminate the wound site.³⁹ Since, 100% ESF has higher VTR and higher PBS uptake, which are essential for wound dressing, it may be considered as a better material among these two polymers.

4. Conclusions

The mats were prepared from 100%ESF and its blend with PLA polymer by the electrospinning process. Tetracycline hydrochloride was added with the polymer solution and was spun into mat. They were characterized for physical, chemical and biological properties which are required for using them as a skin contact layer of multilayer wound dressing system. The electrospun ESF fibres had a mean diameter of 320 nm and ESF-PLA fibres had 502 nm. The FTIR study showed that TCH added with the polymer were present on the mat after electrospinning. Following conclusions are drawn from the study:

- There is no significant change in the coefficient of friction of mat due to incorporation of TCH.
- The surface roughness of mat decreases due to incorporation of TCH
- PBS uptake is lesser for ESF-PLA mat compared to that of 100% ESF mat as the mat become hydrophobic with the incorporation of the PLA
- The contact angle with water is 23° for 100% ESF mat and 79° for ESF-PLA mat.
- The PBS vapor loss across the ESF electrospun mat decreases when PLA is added. The VTR of 100% ESF is also less than the level which would cause dehydration.
- TCH loaded mats show higher zone of inhibition against gram positive bacteria *S. aureus*, *S.epidermidis* and gram negative bacteria *E.coli* compared to that of mat without TCH.
- Cytotoxicity study on neuroblast cells showed that ESF is not inhibiting the growth of cells.
- The *in vivo* wound healing study on rat model showed that the wound dressings developed from 100% ESF with TCH, ESF-PLA with TCH and hydrocolloids show

better healing performance compared to the open wound and conventional gauze cloth wound dressings.

- 100% ESF with TCH mat can be considered a better material, as it possesses higher VTR and higher PBS uptake which are essential for the wound dressing, compared to that of ESF-PLA with TCH mat.

All experiments were performed with the approval of the Institutional Animal Ethics Committee (IAEC) No. KMCRET/Ph.D./06/2013-14.

Acknowledgement

The authors are thankful for the CSIR, India for funding to carry out this research work (Sanction No. 80(0076)/11/EMR - II dated 12.01.2012).

References

- 1 S. Ather and K. G. Harding, in *Advanced Textiles for Wound Care*, ed. S. Rajendran, Woodhead Publishing, 2009, ch.1, pp. 3–19.
- 2 A. M. Reed, *J. Biomater. Appl.*, 1991, 6, 3–41.
- 3 W. Czaja, A. Krystynowicz, S. Bielecki and R. M. Brown Jr., *Biomaterials*, 2006, 27, 145–151.
- 4 W. Paul and C. P. Sharma, *Trends Biomater Artif Organs*, 2004, 18, 18–23.
- 5 F.-H. Lin, T.-M. Chen, K.-S. Chen, T.-H. Wu and C.-C. Chen, *Mater. Chem. Phys.*, 2000, 64, 189–195.
- 6 H.-J. Kim, E.-Y. Choi, J.-S. Oh, H.-C. Lee, S.-S. Park and C.-S. Cho, *Biomaterials*, 2000, 21, 131–141.

- 7 Y. Wang, H.-J. Kim, G. Vunjak-Novakovic and D. L. Kaplan, *Biomaterials*, 2006, 27, 6064–6082.
- 8 C. Vepari and D. L. Kaplan, *Prog. Polym. Sci.*, 2007, 32, 991–1007.
- 9 A. Muthumanickam, S. Subramanian, M. Goweri, W. S. Beaula and V. Ganesh, *Iran. Polym. J.*, 2013, 22, 143–154.
- 10 M. Andiyappan, S. Sundaramoorthy, P. Vidyasekar, N. T. Srinivasan and R. S. Verma, *Int. J. Mater. Res.*, 2013, 104, 498–506.
- 11 W. D. Farrington, J. Lunt, S. Davie, R. S. Blackburn, *In Biodegradable and Sustainable Fibres*. ed. R. S. Blackburn, Woodhead Publishing, 2005, Ch.6, pp. 191–292.
- 12 Y. Wu, M. Li and H. Gao, *J. Polym. Res.*, 2009, 16, 11–18.
- 13 P. Zahedi, I. Rezaeian, S.-O. Ranaei-Siadat, S.-H. Jafari and P. Supaphol, *Polym. Adv. Technol.*, 2010, 21, 77–95.
- 14 A. Frenot and I. S. Chronakis, *Curr. Opin. Colloid Interface Sci.*, 2003, 8, 64–75.
- 15 J.-P. Chen, G.-Y. Chang and J.-K. Chen, *Colloids Surf. Physicochem. Eng. Asp.*, 2008, 313–314, 183–188.
- 16 Y. Zhang, C. T. Lim, S. Ramakrishna and Z.-M. Huang, *J. Mater. Sci. Mater. Med.*, 2005, 16, 933–946.
- 17 A. Muthumanickam, E. Elankavi, R. Gayathri, S. K. Sampathkumar, G. Vijayakumar, K. Muthukumar and S. Subramanian, *Int. J. Mater. Res.*, 2010, 101, 1548–1553.

- 18 K. J. Quinn, J. M. Courtney, J. H. Evans, J. D. Gaylor and W. H. Reid, *Biomaterials*, 1985, 6, 369–377.
- 19 T. Maneerung, S. Tokura and R. Rujiravanit, *Carbohydr. Polym.*, 2008, 72, 43–51.
- 20 S. T. Thomas, in *Advanced Textiles for Wound Care*, ed. S. Rajendran, Woodhead Publishing, 2009, ch.2, pp. 20–47.
- 21 ASTM Standards E96-00. Standard test methods for water vapour transmission of materials. *Annual book of ASTM standards*, vol.4.06. Philadelphia: ASTM;2000.
- 22 F.-L. Mi, Y.-B. Wu, S.-S. Shyu, A.-C. Chao, J.-Y. Lai and C.-C. Su, *J. Membr. Sci.*, 2003, 212, 237–254.
- 23 E. K. Mooney, C. Lippitt and J. Friedman, *Plast. Reconstr. Surg.*, 2006, 117, 666–669.
- 24 Y. Chen, L. Yan, T. Yuan, Q. Zhang and H. Fan, *J. Appl. Polym. Sci.*, 2011, 119, 1532–1541.
- 25 V. Sarath Chandra, Ganga Baskar, R. V. Suganthi, K. Elayaraja, M. I. Ahymah Joshy, W. Sofi Beaula, R. Mythili, Ganesh Venkatraman, S. Narayana Kalkura, *ACS Appl. Mater. Interfaces*, 2012, 4, 1200–1210.
- 26 C. Gu and K. G. Karthikeyan, *Environ. Sci. Technol.*, 2005, 39, 2660–2667.
- 27 J. Coates, in *Encyclopedia of Analytical Chemistry*, John Wiley & Sons, Ltd, 2006.
- 28 Y. J. Yeul Woo, *J Ind Eng Chem*, 2007, 13, 457–464.
- 29 C.-L. He, Z.-M. Huang and X.-J. Han, *J. Biomed. Mater. Res. A*, 2009, 89A, 80–95.

- 30 A. Mg, C. R. N, H. N. M and P. P, *Asian J. Pharm.*, 2009, 3, 113.
- 31 P. Wu, A. C. Fisher, P. P. Foo, D. Queen and J. D. S. Gaylor, *Biomaterials*, 1995, 16, 171–175.
- 32 B. Balakrishnan, M. Mohanty, P. R. Umashankar and A. Jayakrishnan, *Biomaterials*, 2005, 26, 6335–6342.
- 33 Fwu-Long Mi, Shin-Shing Shyu, Yu-Bey Wu, Sung-Tao Lee, Jen-Yeu Shyong, Rong-Nan Huang, *Biomaterials*, 2001,22, 165-173.
- 34 D. Queen, J. D. S. Gaylor, J. H. Evans, J. M. Courtney and W. H. Reid, *Biomaterials*, 1987, 8, 367–371.
- 35 A. W. Bauer, W. M. Kirby, J. C. Sherris and M. Turck, *Am. J. Clin. Pathol.*, 1966, 45, 493–496.
- 36 *Performance Standards for Antimicrobial Disk Susceptibility Test*, M100-S22, CLSI Vol. 32 No. 3. Jan 2012
- 37 P. Zahedi, Z. Karami, I. Rezaeian, S.-H. Jafari, P. Mahdaviani, A. H. Abdolghaffari and M. Abdollahi, *J. Appl. Polym. Sci.*, 2012, 124, 4174–4183.
- 38 L. Amalorpava Mary, T. Senthilram, S. Suganya, L. Nagarajan, J. Venugopal, S. Ramakrishna, V. R. Giri Dev, *Express Polym Lett*, 2013, 7, 238–48.
- 39 Andrew M. Reed, *J. Biomater. Appl.*, 1991, 6(1), 3-41.

Figure Captions

Fig. 1a) SEM Image of 100% ESF mat

Fig. 1aa) Fibre diameter histogram of 100% ESF mat

Fig. 1b) SEM Image of ESF-PLA mat

Fig. 1bb) Fibre diameter histogram of ESF-PLA mat

Fig. 1c) SEM image of TCH incorporated ESF mat

Fig. 1cc) Fibre diameter histogram of TCH incorporated ESF mat

Fig. 1d) SEM image of TCH incorporated ESF-PLA mat

Fig. 1dd) Fibre diameter histogram of TCH incorporated ESF-PLA mat

Fig. 2 FTIR spectra of a) 100% PLA mat, b) TCH powder, c) PLA with TCH mat, d) 100% ESF mat and e) ESF with TCH mat

Fig. 3 Phosphate Buffered Saline uptake of 100% ESF and ESF-PLA mat

Fig. 4 a) Contact angle of ESF-PLA mat

Fig. 4 b) Contact angle of 100% ESF mat

Fig. 5 PBS loss in 100% ESF and ESF-PLA mat

Fig. 6 Antibacterial activity against Gram positive bacteria (A1, A2, A3 - 1%, 2% and 3% (w/v) of TCH in 100% ESF; C is the control 100% ESF mat without TCH)

Fig. 7 Antibacterial activity against Gram negative bacteria (B1, B2, B3 - 1%, 2% and 3% (w/v) of TCH in ESF-PLA mats; C is the control ESF-PLA mat without TCH)

Fig. 8 Cell viability

Fig. 9 a) 2NA cells on 100% ESF mat

Fig. 9 b) Hematoxylin 20X on 100% ESF mat

Fig. 9 c) Toluidine blue 20X on 100% ESF mat

Fig. 10 Representative photographs of macroscopic appearance of the experimental wound healing in 0-17 days

Fig. 11 Histopathological photographs of Group1 wound on (a) 3rd, (b) 7th and (c) 11th day of postoperation

Fig. 12 Histopathological photographs of Group2 wounds on (a) 3rd, (b) 7th and (c) 11th day of postoperation

Fig. 13 Histopathological photographs of Group3 wounds on (a) 3rd, (b) 7th and (c) 11th day of postoperation

Fig. 14 Histopathological photographs of Group4 wounds on (a):3rd (b):7th and (c):11th day of postoperation

Fig. 15 Histopathological photographs of Group5 wounds on a) 3rd, (b) 7th and (c) 11th day of postoperation

Fig. 16 Histopathological photographs of Group6 wounds on (a) 3rd, (b) 7th and (c) 11th day of postoperation

Table Captions

Table 1 Surface roughness of 100% ESF with TCH and without TCH mats

Table 2 Antimicrobial activity of TCH loaded nano fibrous mats

Table 3 Hemolysis percentage of 100% ESF and ESF-PLA mats with TCH and without TCH

Table 4 Contraction (%) in wound area on 3,5,7,9,11,13,15 and 17th day of postoperation

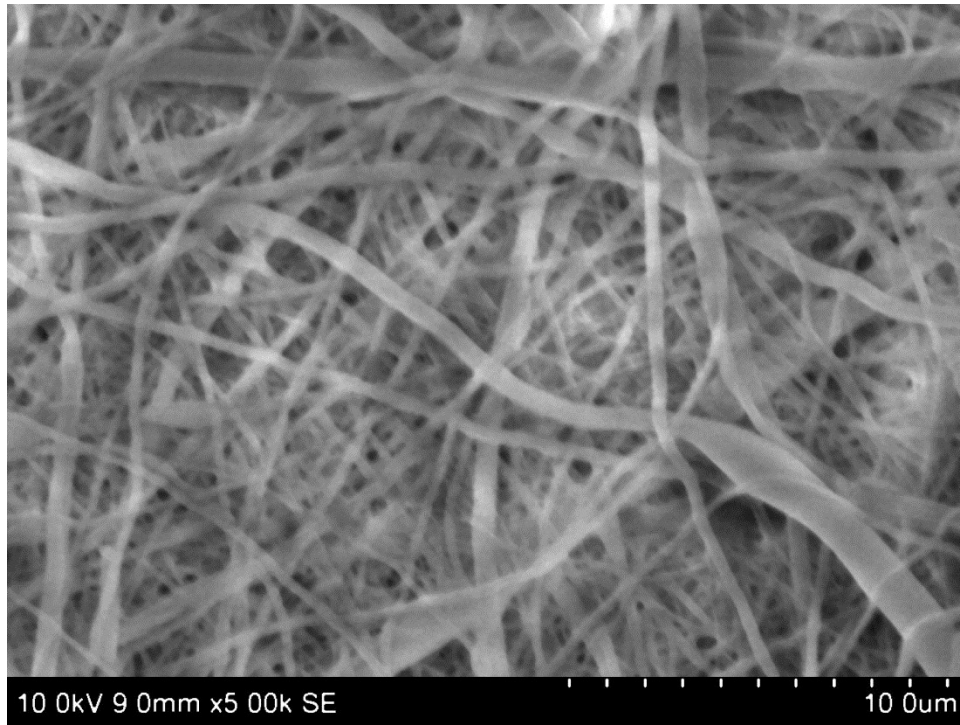


Fig. 1a

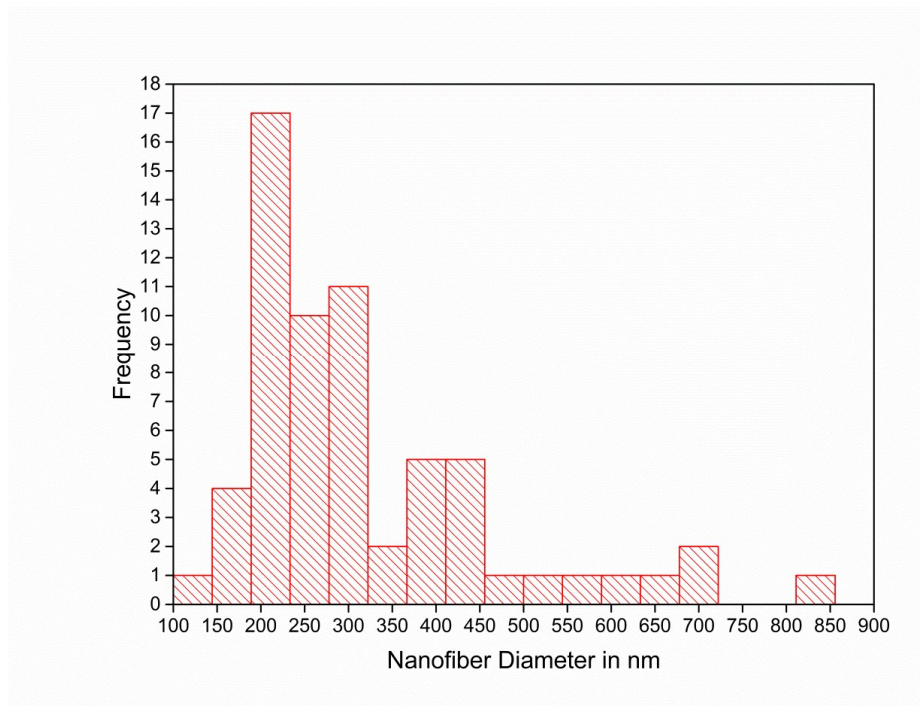


Fig. 1aa

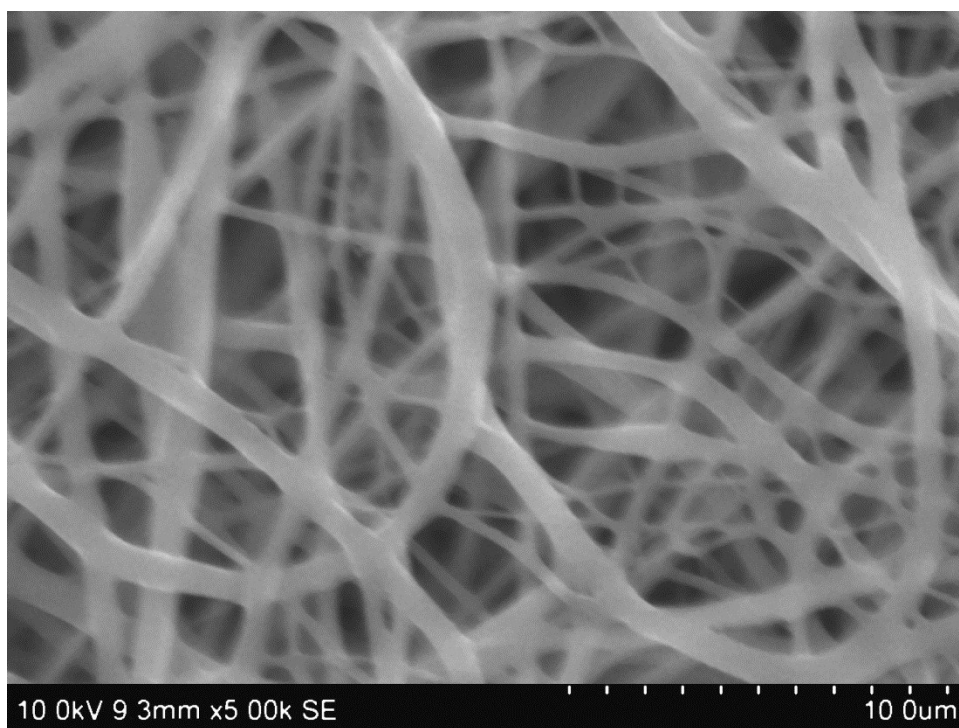


Fig. 1b

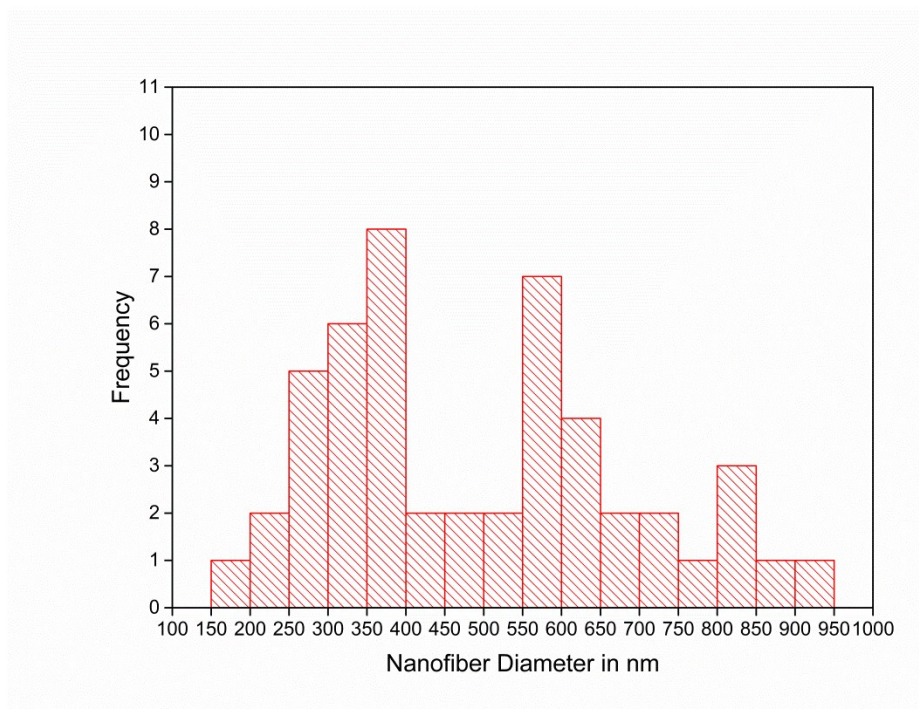


Fig. 1bb

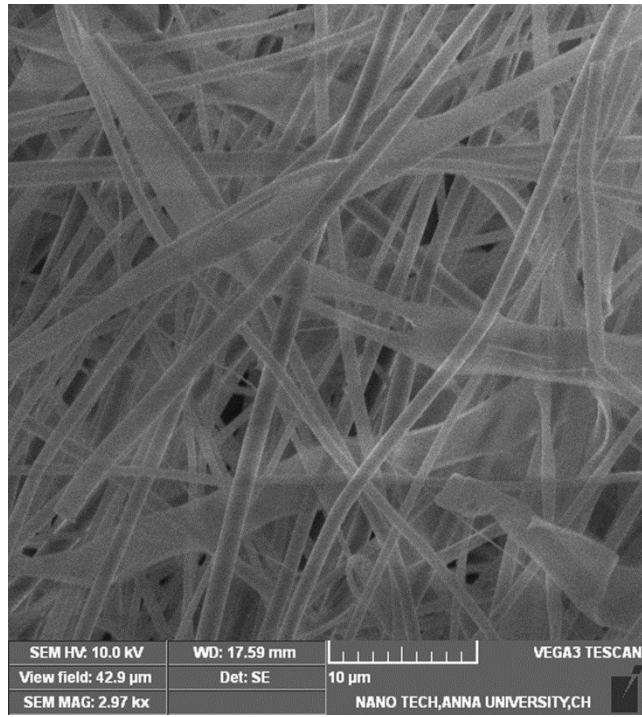


Fig. 1c

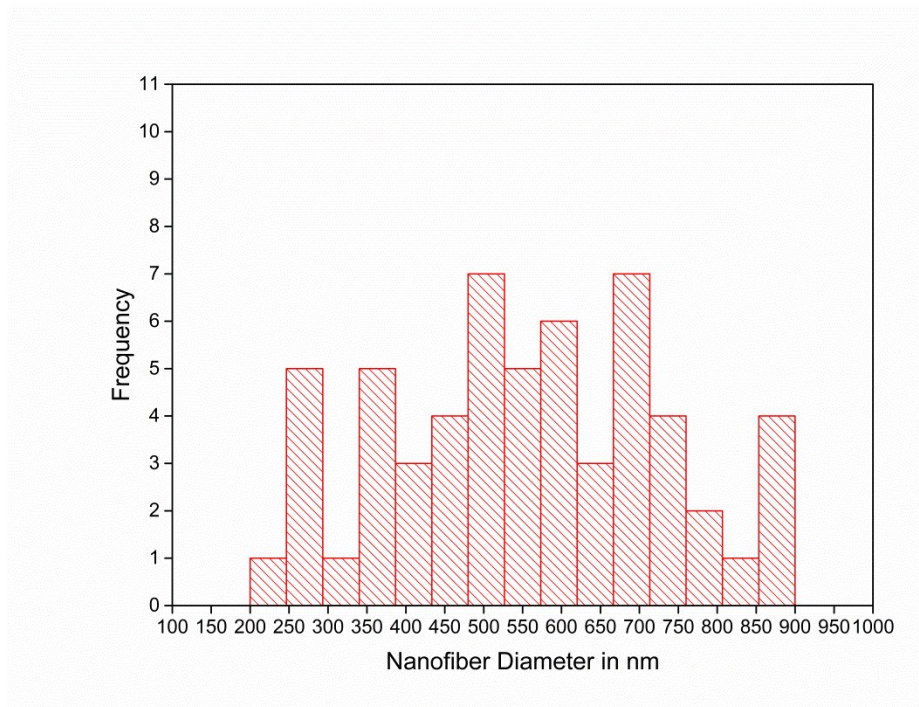


Fig. 1cc

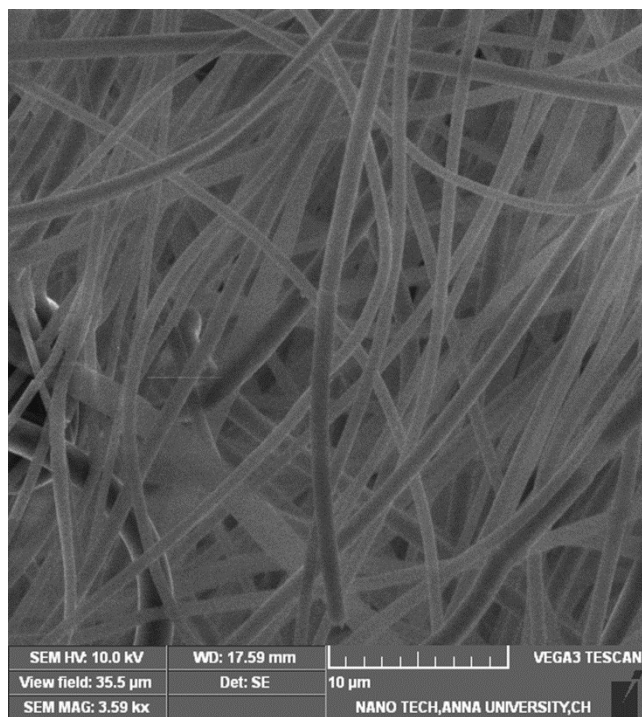


Fig. 1d

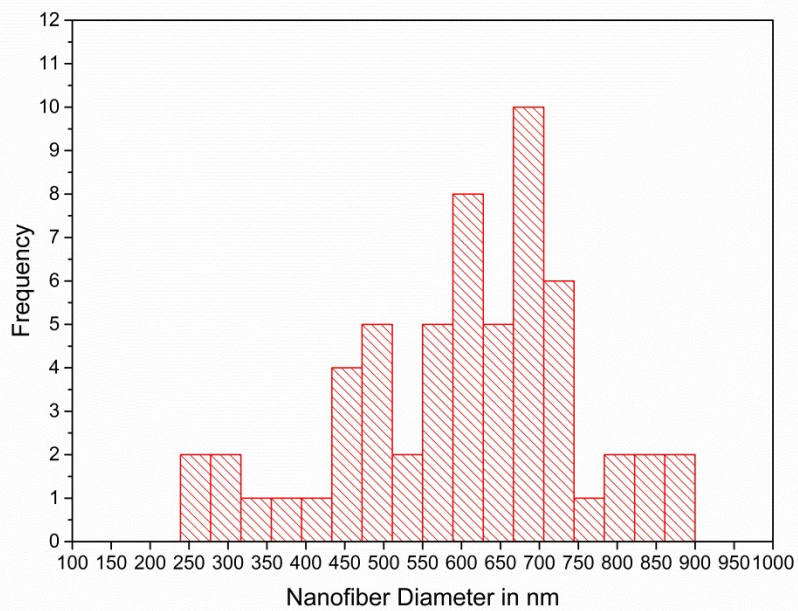


Fig. 1dd

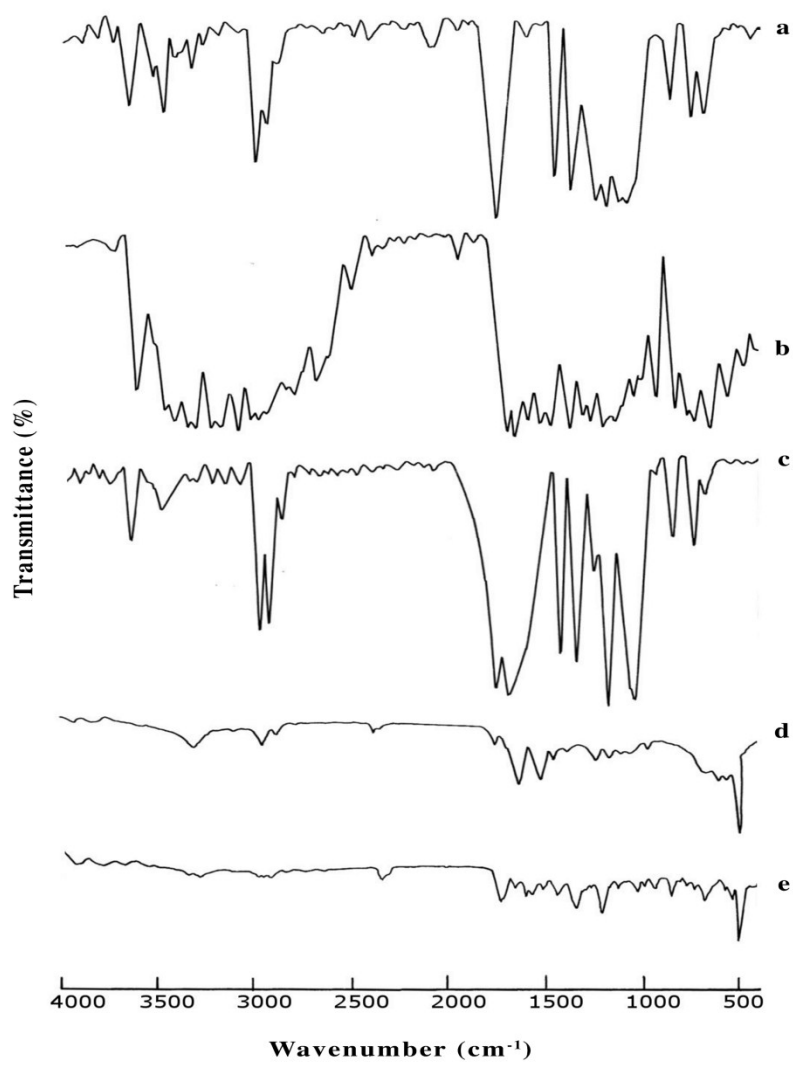


Fig. 2

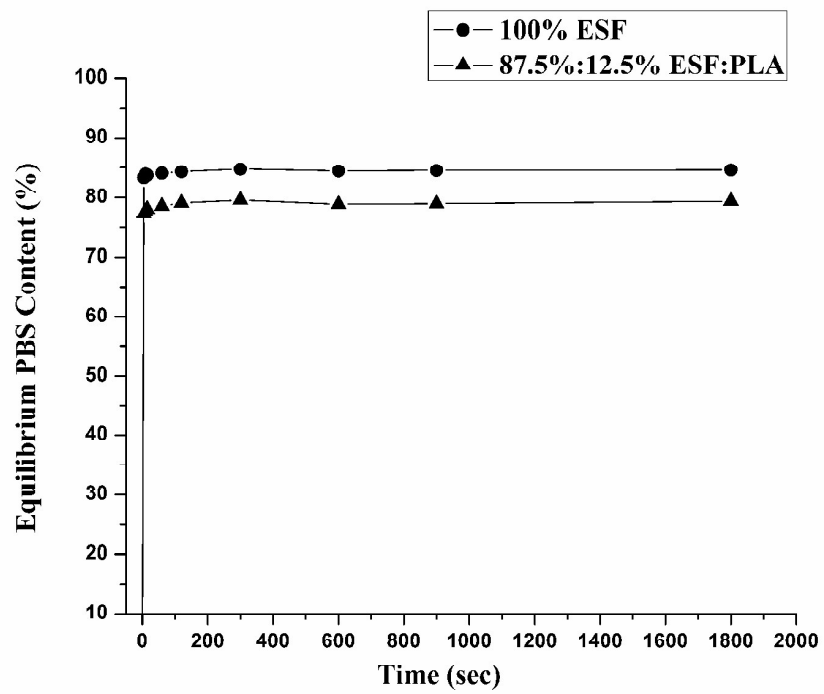


Fig. 3

(a)



Fig. 4a

(b)

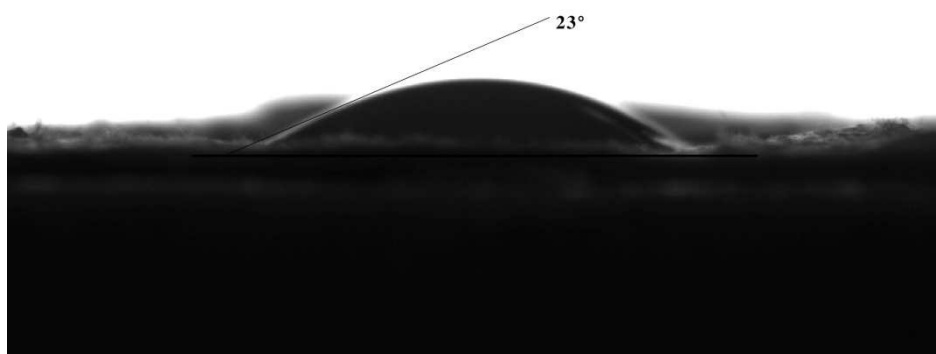


Fig. 4b

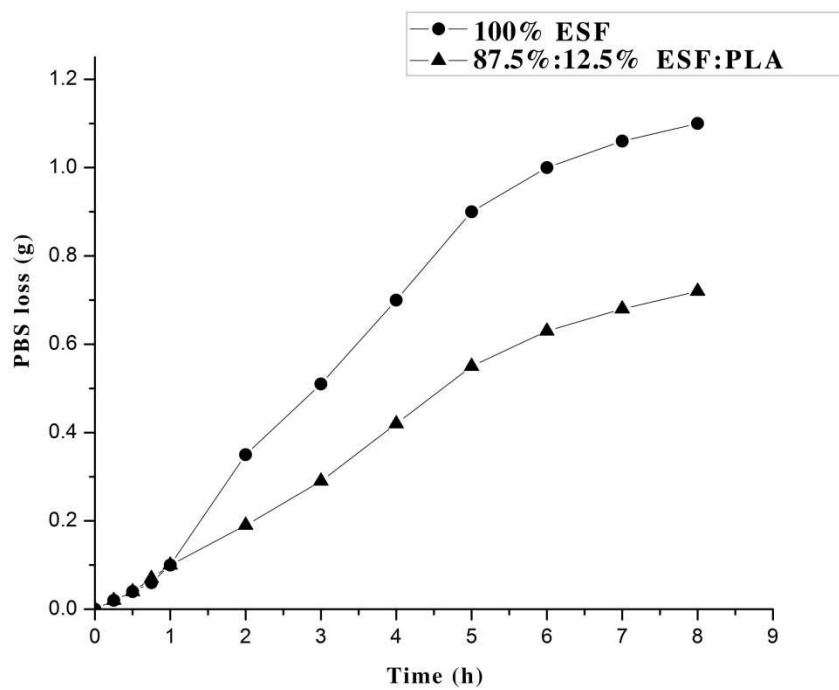


Fig.5

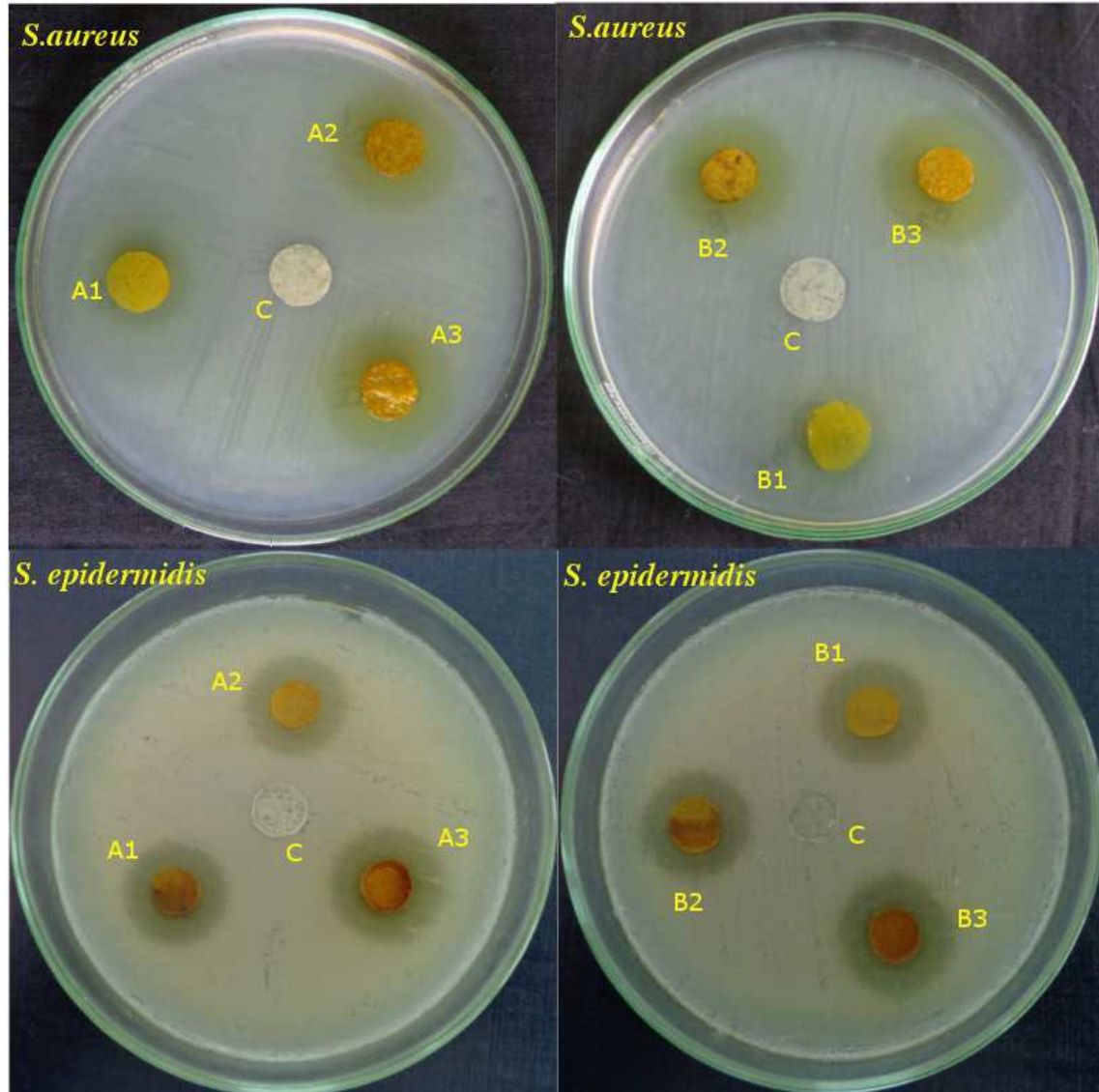


Fig.6

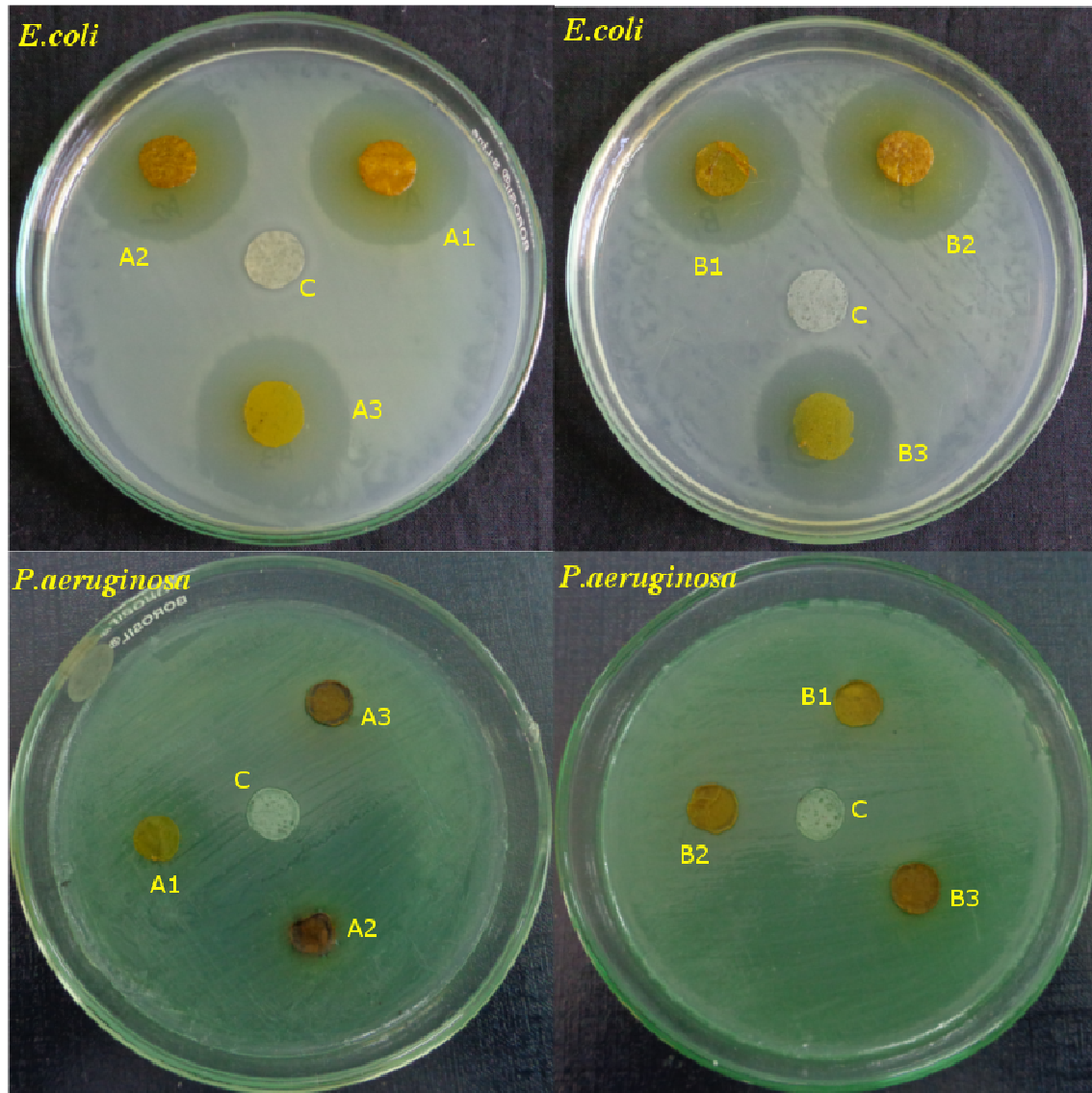


Fig.7

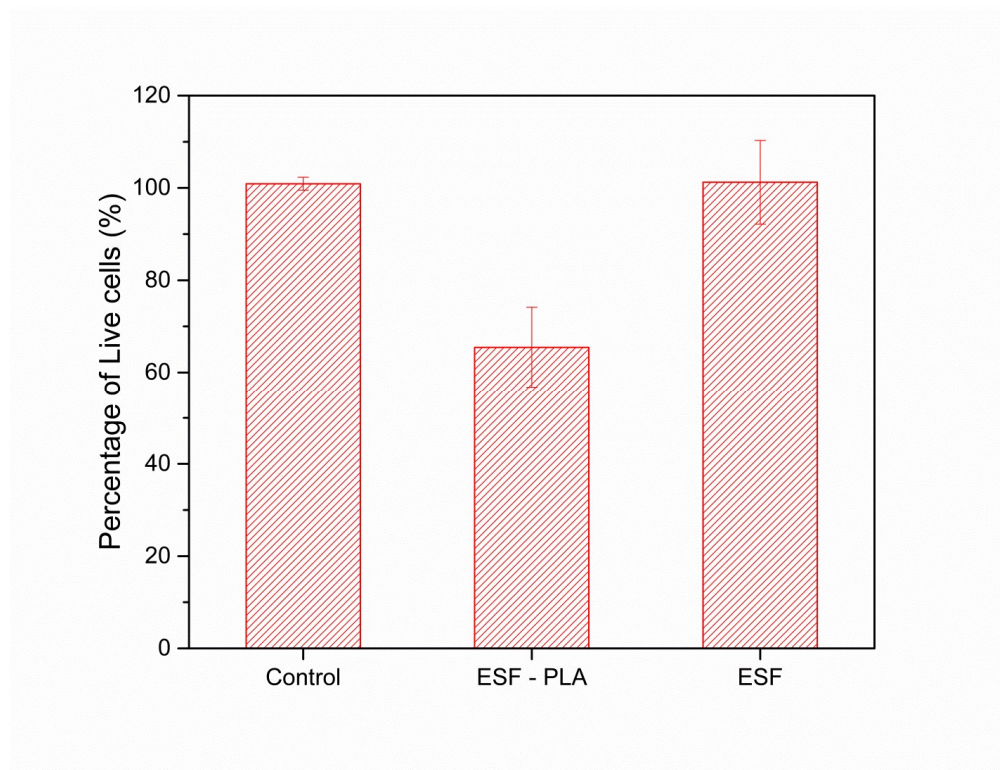


Fig.8

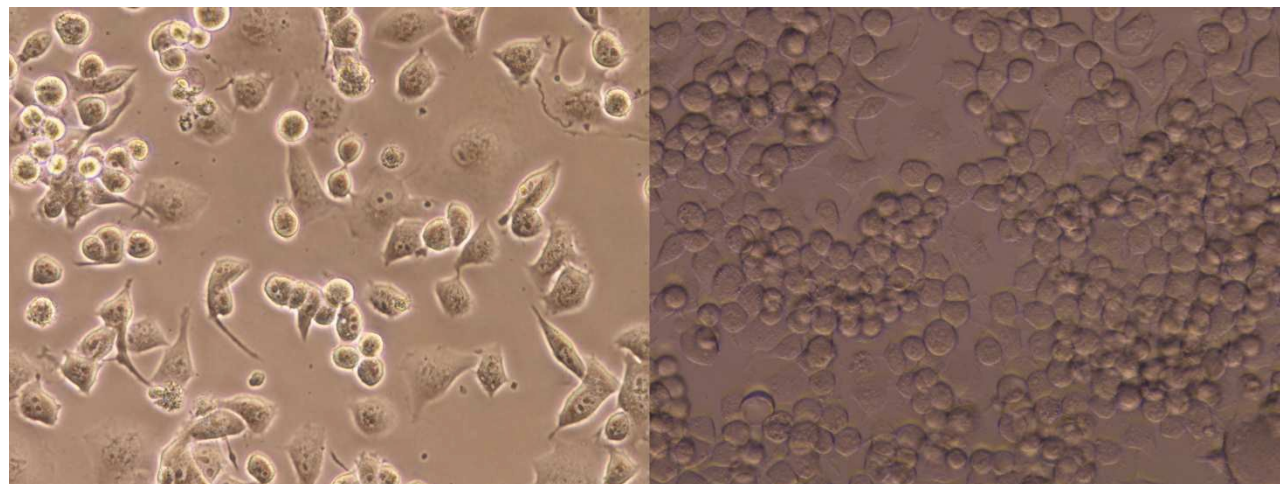


Fig.9a

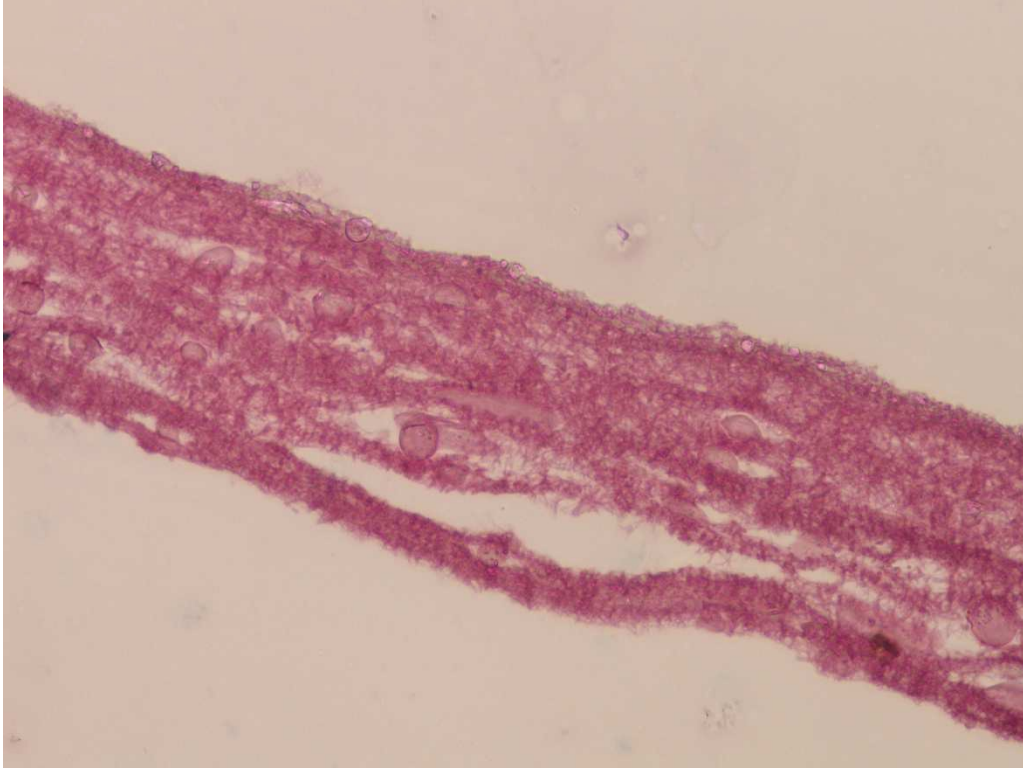


Fig.9b

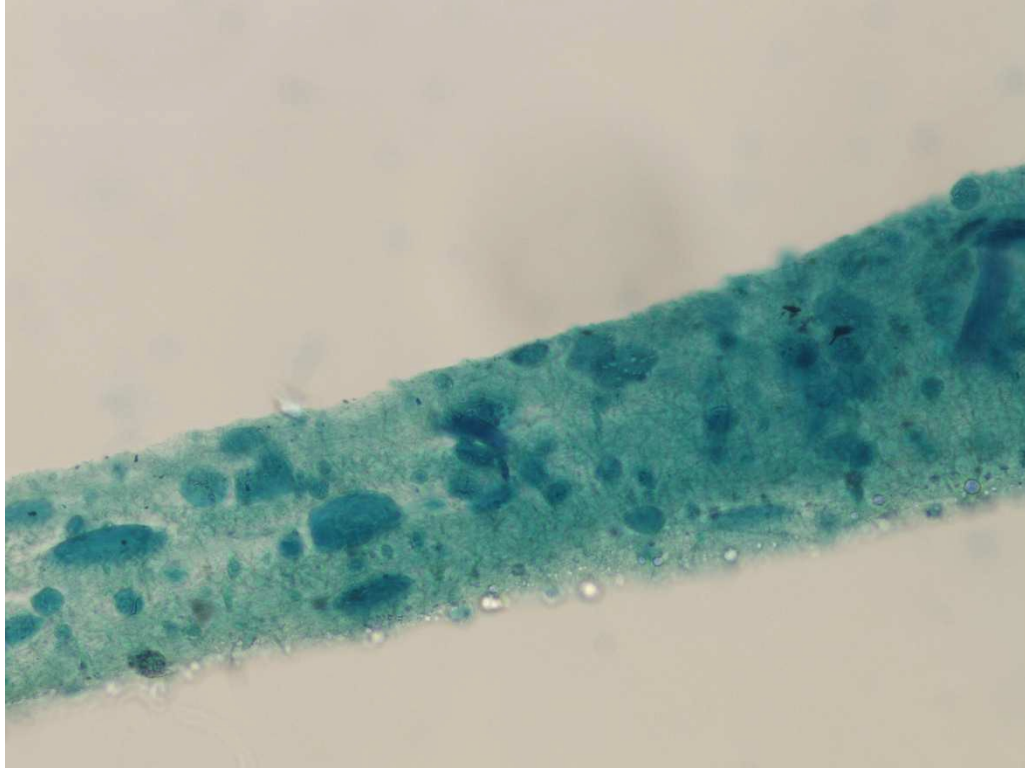


Fig.9c

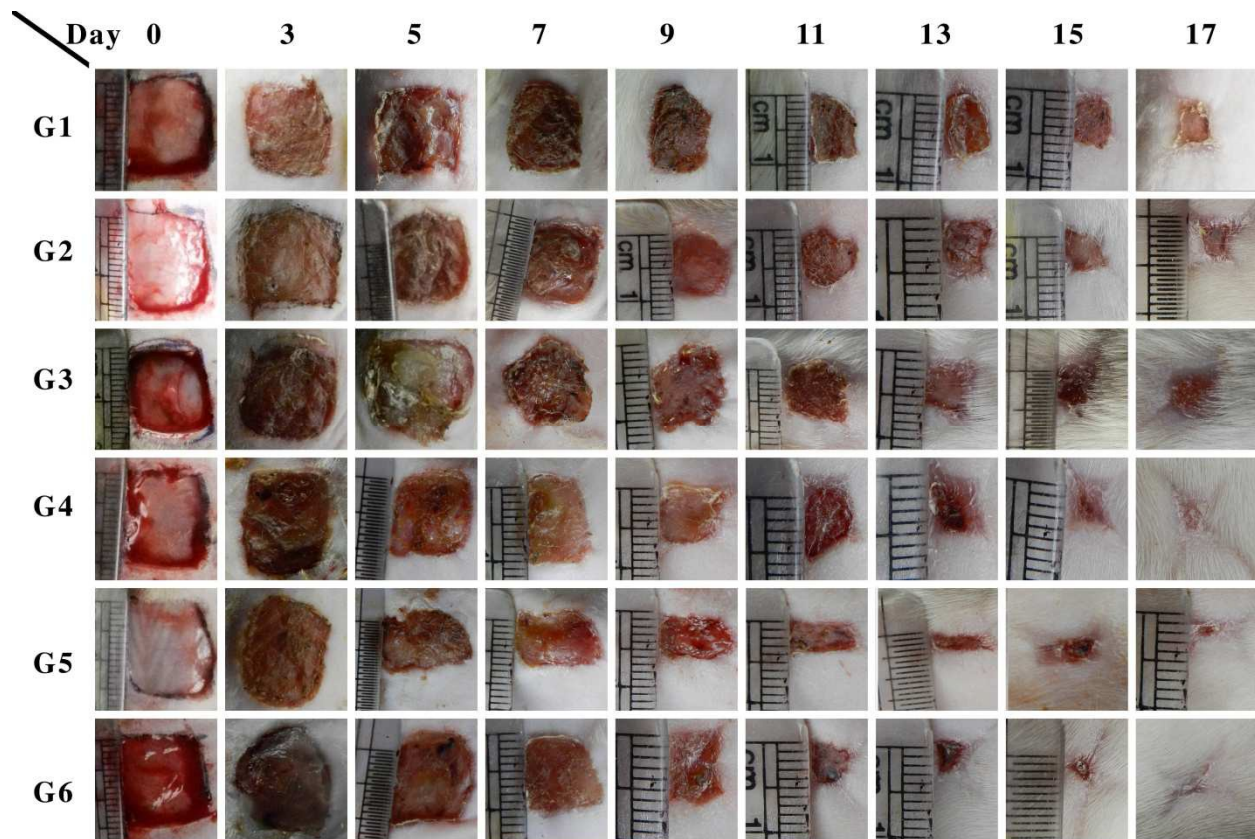


Fig.10

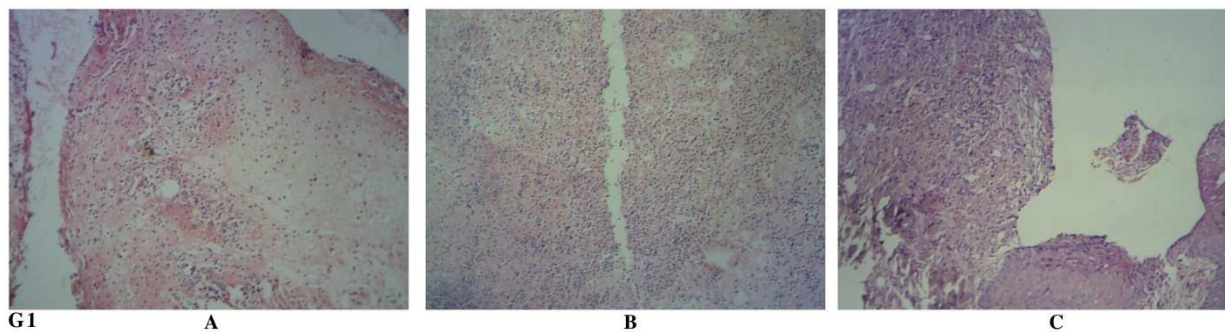


Fig.11

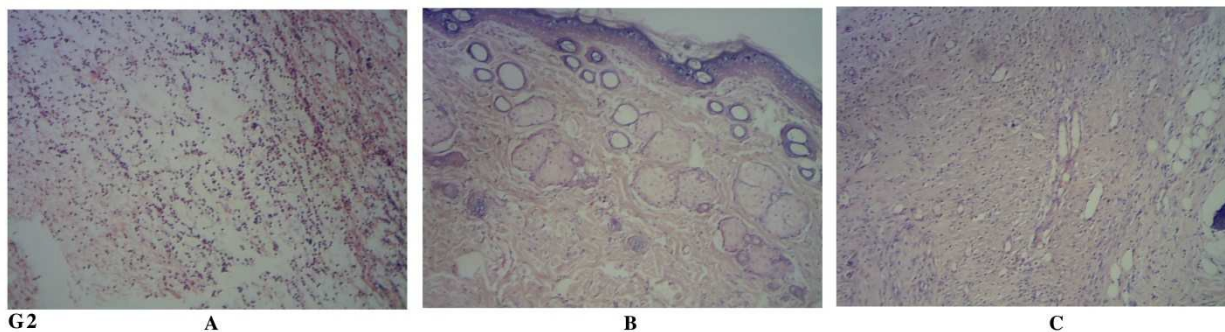


Fig.12

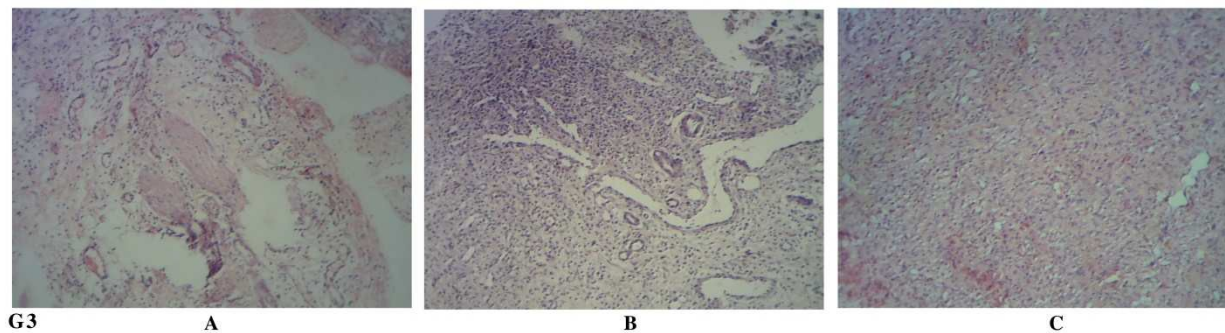


Fig.13

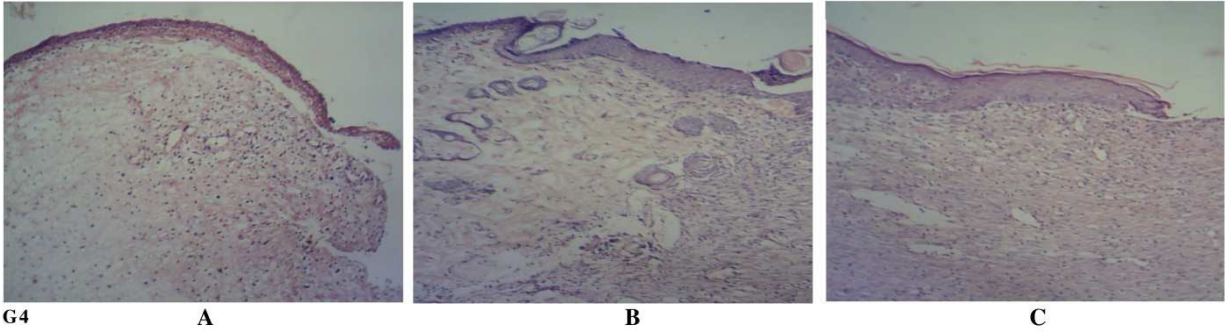


Fig.14

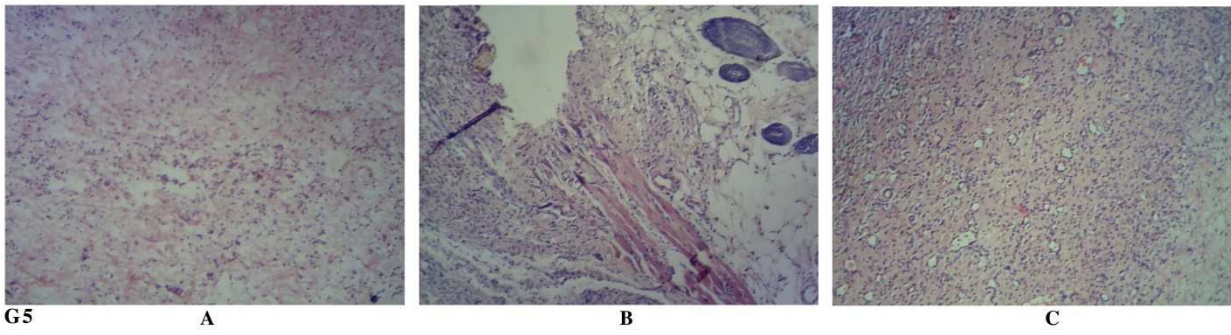


Fig.15

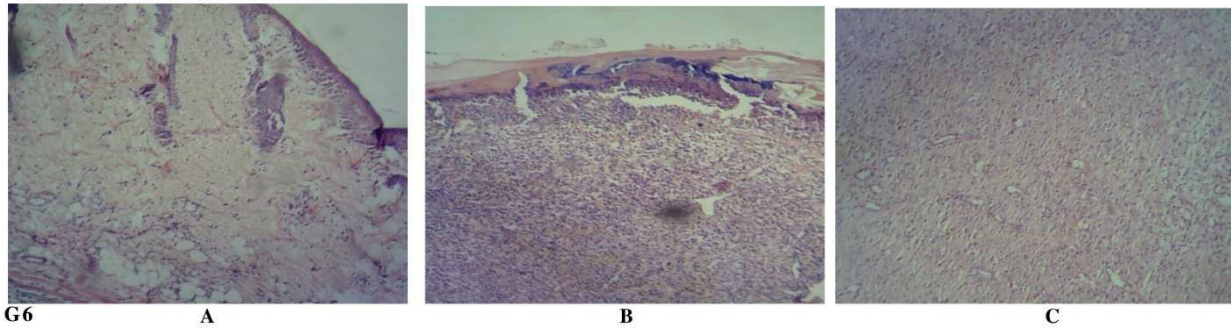


Fig.16

Table 1 Surface roughness of 100%ESF with TCH and without TCH mats

S. No	With drug			Without drug		
	MIU*	MMD*	SMD*	MIU	MMD	SMD
1	0.52	0.54	1.02	0.46	0.58	2.91
2	0.68	0.6	1.1	0.54	0.78	3.83
3	0.6	0.52	0.98	0.5	0.62	3.24
4	0.46	0.58	0.92	0.42	0.62	3.28
5	0.78	0.62	0.87	0.62	0.55	2.73
6	0.43	0.52	0.95	0.43	0.58	1.98
7	1.02	0.7	0.83	0.52	0.54	2.42
8	0.3	0.8	0.76	1.08	0.68	3.84
9	0.48	0.56	0.73	0.97	0.81	3.51
10	0.52	0.6	0.81	1.07	0.91	3.15
11	1.18	0.96	0.72	0.26	0.72	3.24
12	0.4	0.48	0.68	0.25	0.88	4.24
13	0.63	0.68	0.68	0.68	0.62	2.32
14	0.52	0.72	0.81	0.58	0.8	3.1
15	0.49	0.65	0.78	0.76	0.72	2.9
Mean	0.60	0.64	0.84	0.61	0.69	3.11
SD	0.236	0.125	0.128	0.262	0.12	0.607

*MIU - Mean Co efficient of Friction, MMD- Mean Deviation for MIU, SMD- Surface Roughness

Table 2 Antimicrobial activity of TCH loaded nano fibrous mats

S. No.	Organisms	Antimicrobial activity (zone of inhibition (ZOI) in mm)						
		Control Sample	100 % ESF			ESF-PLA		
			TCH concentration			TCH concentration		
			1%	2%	3%	1%	2%	3%
1	<i>Staphylococcus aureus</i>	0	16.33*, 0.57**	24.33, 1.15	27.33, 1.15	16, 1	23.33, 0.57	24.33, 0.57
2	<i>Staphylococcus epidermidis</i>	0	15, 1	19, 1	20.66, 0.57	15.33, 0.57	18.66, 0.57	22.33, 1.15
3	<i>Escherichia coli</i>	0	23.66, 1.15	26, 1	29.33, 1.15	24.66, 1.15	26.33, 0.57	27.66, 0.57
4	<i>Pseudomonas aeruginosa</i>	0	0	0	0	0	0	0

* mean, **standard deviation

Table 3 Hemolysis percentage of 100% ESF and ESF-PLA mats with TCH and without TCH

Sample	Hemolysis%	
	Mean	SD
100% ESF without TCH	0.346	0.020
100% PLA without TCH	0.319	0.021
ESF-PLA without TCH	0.356	0.020
100% ESF with 1% of TCH	0.352	0.015
100% ESF with 2% of TCH	0.459	0.038
100% ESF with 3% of TCH	0.566	0.040
ESF-PLA with 1% of TCH	0.382	0.021
ESF-PLA with 2% of TCH	0.566	0.036
ESF-PLA with 3% of TCH	0.676	0.026

Table 4 Contraction (%) in wound area on 3,5,7,9,11,13,15 and 17th day of postoperation

Groups	Days of postoperation							
	3	5	7	9	11	13	15	17
1	-2*, 0.31**	2, 0.36	14, 0.35	28, 2.21	37, 0.816	52, 1.48	61, 1.52	72, 2
2	-3.02, 0.16	2.90, 0.19	16.62, 0.39	27.12, 0.43	35.16, 0.70	52.85, 0.17	57.59, 0.278	73, 0.29
3	4.47, 0.56	2.37, 0.32	16.76, 0.21	32.47, 1.42	45.5, 0.47	52, 0.55	60.25, 1.18	75.8, 0.77
4	6.22, 0.43	16.28, 0.4	32.15, 1.4	44.6, 0.44	57.3, 0.50	67.7, 1.20	83.5, 0.73	95, 2.70
5	5.69, 0.36	16, 0.22	30, 0.50	40, 0.89	56, 1.50	70, 0.67	83, 0.95	95.9, 0.70
6	7.75, 0.66	18.8, 1.06	29.4, 0.75	36, 1.16	60, 1.59	70.6, 1.18	82.3, 0.55	96.8, 1.73

* mean, ** standard deviation